14

Buckling of beams

When a structure is subjected to loading, it can fail because local stresses exceed the maximum allowable stress for the material. There exist, however, another type of failure mode where the entire structure suddenly collapses. The critical value of the applied load that triggers this failure mode primarily depends on the geometry of the structure and the stiffness of the material, not its strength. The study of this catastrophic failure mode is known as the theory of *elastic stability*.

The best known problem of elastic stability undoubtedly is the transverse buckling of a beam. Consider a straight cantilevered beam subjected to an end axial compressive load. If this load is applied at the centroid of the cross-section of the beam, it creates only an axial straining of the beam. As the axial compressive load is increased, a critical value is reached when the beam buckles sideways and collapses.

The basic concepts involved in the study of elastic stability will be introduced with the simple problem of a rigid bar with a root torsional spring subjected to a compressive load. This will serve as an introduction to the problem of buckling of beams. Beams, when subjected to compressive axial loads, are often called *columns*, although this designation will not be used in this text.

14.1 Rigid bar with root torsional spring

14.1.1 Analysis of a perfect system

Consider a rigid bar of length L articulated at the root as depicted in fig. 14.1. A torsional spring of constant k is acting at the root, and is un-stretched when the bar is vertical. A compressive axial load, P, constantly acting in the vertical direction, is applied at the bar's tip. Let the lateral deflection of the bar be defined by angle θ measured from the vertical. The equilibrium of moments about point **O** implies

$$M - k\theta = 0, \tag{14.1}$$

where M is the moment of the applied load, and $k\theta$ the elastic restoring force in the spring. The moment of the applied load is $M = PL\sin\theta$ resulting in the following

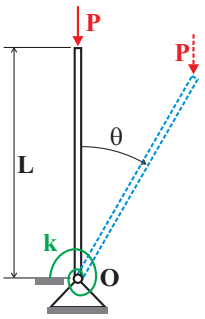

Fig. 14.1. Bar with a root torsional spring.

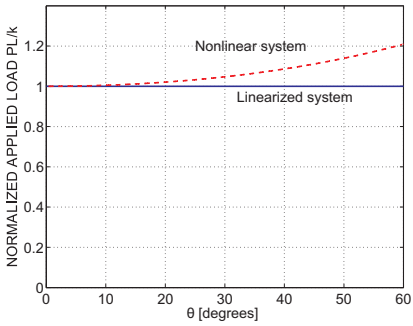

Fig. 14.2. Behavior of a perfect system.

equilibrium equation

$$PL\sin\theta - k\theta = 0 \tag{14.2}$$

In the theory of elastic stability, the determination of the critical load for the onset of instability plays a central role. Since the elastic spring is un-stretched when $\theta = 0$, the rigid bar will remain vertical as the applied load P is increased. At the onset of buckling, the bar will start to move sideways and θ will increase. If the onset of buckling is to be determined, angle θ can be assumed to be a small quantity,

$$\sin\theta \approx \theta. \tag{14.3}$$

Hence, eq. (14.2) becomes

$$(PL - k)\theta = 0 \tag{14.4}$$

This equation of equilibrium is satisfied if $\theta = 0$. This represents, however, the trivial solution where the bar remains vertical. Indeed, when the bar is vertical, the line of action of the applied force passes through point **O**, the moment in the spring vanishes, and equation (14.1) is then identically satisfied for any value of the applied load, P.

An important point is to determine whether equation (14.4) admits a non-trivial solution. In fact, the *buckling load*, sometimes called the *critical load* of the system and denoted $P_{\rm cr}$, is defined as that load for which a non-trivial solution of eq. (14.4) exists. Clearly, if $(PL - k) = 0$,

$$P_{\rm cr} = \frac{k}{L}. \tag{14.5}$$

When $P = P_{\rm cr}$, equation of equilibrium, eq. (14.4), is satisfied for an arbitrary value of angle θ. The behavior of the system is depicted in fig. 14.2. For $P < P_{\rm cr}$, the only solution of eq. (14.4) is $\theta = 0$. When the applied load reaches the buckling load, *i.e.*, when $P = P_{\rm cr}$, another solution of eq. (14.4) exists for which angle θ is arbitrary, and this is shown by the horizontal line labeled "linearized system."

Strictly speaking, the solution described in fig. 14.2 is only valid for small θ, because assumption (14.3) is made. When θ becomes large, the post-buckling range starts, and eq. (14.2) must be used. This equation is recast as

$$\frac{P}{P_{\text{cr}}} = \frac{\theta}{\sin\theta} \tag{14.6}$$

This nonlinear relationship is also depicted in fig. 14.2. Both linearized and nonlinear solutions are in close agreement for small angles. The buckling load characterizes the onset of buckling, *i.e.*, the loading for which lateral displacement begins.

From a design standpoint, it is often imperative to keep the applied load well below the buckling load, because the collapse of the structure at the buckling load is a sudden and catastrophic phenomenon. The buckling load depends on k, the spring stiffness constant, and L, the length of the bar. The strength of the system components are irrelevant in this analysis.

14.1.2 Analysis of an imperfect system

The system considered above is a *perfect system* in the sense that the rigid bar is perfectly straight, the line of action of the applied load exactly passes through the pivot point, and the un-stretched position of the spring corresponds to $\theta = 0$. In practical situations, however, a certain level of *imperfection* is always present. The actual imperfection of the system is often unknown, as it comes from manufacturing inaccuracies or load misalignment.

A convenient way of introducing imperfection in the system is to assume that the un-stretched position of the spring corresponds to $\theta = \theta_0$, where θ_0 is now a measure of the initial imperfection of the system. The equilibrium eq. (14.2) then becomes

$$PL\sin\theta - k(\theta - \theta_0) = 0. \tag{14.7}$$

The onset of buckling can be determined assuming θ to be a small quantity, implying (14.3), to find

$$(PL - k)\theta = -k\theta_0. \tag{14.8}$$

This equation possesses a non-vanishing right-hand side, in contrast with the homogeneous equation, eq. (14.2), for the perfect system. The solution of eq. (14.8) is

$$\theta = \frac{\theta_0}{1 - P/P_{\text{cr}}} \tag{14.9}$$

The response of the system is very different from that of the perfect system and is depicted in fig. 14.3 for various levels of the initial imperfection, θ_0. Unlike the perfect system, rotation of the bar begins from the onset of loading and grows as the load is increased. When the initial imperfection is very small, the response of the system is very small except when the applied load approaches P_{cr}. When the applied load reaches P_{cr} the response rapidly grows to infinity. For larger initial imperfections, a large response of the system is observed even for applied loads well below the critical load.

In all cases, the response of the system is unbounded when the applied load approaches the buckling load, P_{cr}. In fact, the buckling load can be defined as the load for which the response of an initially imperfect system grows without bounds.

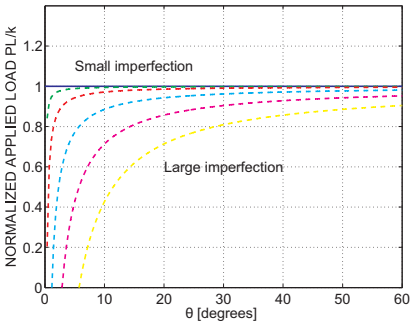

Fig. 14.3. System linearized response with various levels of imperfection.

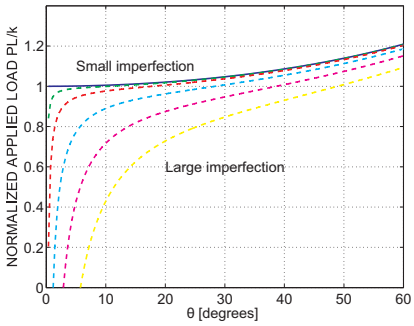

Fig. 14.4. System nonlinear response with various levels of imperfection.

For the simple system discussed here, the analysis of both *perfect* and *imperfect* systems give the same buckling load, eq. (14.5).

The analysis developed here is valid for small values of θ. For larger values of θ equation (14.7) must be used. It can be recast as

$$\frac{P}{P_{\rm cr}} = \frac{\theta - \theta_0}{\sin\theta} \tag{14.10}$$

This relationship is depicted in fig. 14.4 for various levels of the initial imperfection. For angles less than 10 degrees, the curves are nearly identical to those in fig. 14.3, but as the angle increases, the curves bend upwards and asymptotically approach the behavior of the perfect system at large angles as shown in fig. 14.2

Although the buckling loads obtained for the *perfect* and *imperfect* systems are the same, their respective behaviors are quite different for applied loads below the buckling load. Indeed, comparing figs. 14.2 and 14.3 shows that the *perfect* system presents no lateral deflection for applied loads below $P_{\rm cr}$, whereas the *imperfect* system presents lateral deflections even for small applied load. Failure can occur for applied loads far smaller that the buckling load. Assuming that the spring fails when $\theta = \theta_{\rm fail}$, the failure load is readily computed from eq. (14.9) as

$$\frac{P_{\rm fail}}{P_{\rm cr}} = 1 - \frac{\theta_0}{\theta_{\rm fail}}. \tag{14.11}$$

Note the fundamental difference between the failure load associated with a displacement or stress reaching an allowable limit for the material ($\theta = \theta_{\rm fail}$ in this simple example), and the buckling load associated with the instability of a structure, which depends solely on its elastic and geometric characteristics.

In this simple example, two conceptually different definitions of the buckling load are given. First, the buckling load is defined as the critical load for which a *perfect* system admits a non-trivial solution. Second, the buckling load is defined as the load for which the response of an *imperfect* system grows without bounds. Although conceptually different, these two definitions give the same value of the buckling load for the simple rigid bar problem considered here.

14.2 Buckling of beams

Consider now the simply-supported, uniform beam acted upon by a compressive load, P, depicted in fig. 14.5. This loading is assumed to be applied exactly at the centroid of the section. According to three dimensional beam theory, all the conditions for decoupling the problem are met. This means that three simpler, independent problems can be solved: first, an extensional problem giving rise to extension of the beam (compression in this case), and second, two uncoupled bending problems along the principal axes of bending. Because the axial load is applied exactly at the centroid and no transverse loads are applied, the beam does not bend. Consequently, the transverse deflections will remain zero, independently of the level of the applied axial load P.

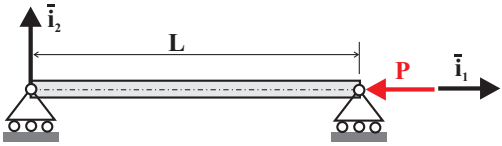

Fig. 14.5. Simply-supported beam with end compressive load.

This simple reasoning shows that the beam theory developed in the previous chapters is unable to predict the buckling phenomenon. The basic equations of Euler-Bernoulli beam theory, eqs. (5.19), and (5.40) must be modified to account for the effect of the large compressive load that causes the instability. The key to this modification is a restatement of the equilibrium equations for a deformed configuration of the beam.

14.2.1 Equilibrium equations

Consider an infinitesimal slice of the beam subjected to axial and transverse forces, as well as bending moments. In contrast with earlier developments, see sections 5.4.3 or 5.5.3, a free body diagram of a *deformed slice of the beam* will be analyzed. Figure 14.6 shows the deformed slice of the beam subjected to the same force and moment components considered in chapter 5. At the onset of buckling, a large axial force is present in the beam, but the transverse shear force and deflection are still very small. Consequently, the following assumption will be made

$$N_1 \gg V_2; \quad \frac{\mathrm{d}\bar{u}_2}{\mathrm{d}x_1} \ll 1. \tag{14.12}$$

The first equilibrium equation is obtained by summing up forces along axis $\bar{\imath}_1$ to find

$$-N_1 \cos\frac{\mathrm{d}\bar{u}_2}{\mathrm{d}x_1} + \left(N_1 + \frac{\mathrm{d}N_1}{\mathrm{d}x_1}\mathrm{d}x_1\right)\cos\left(\frac{\mathrm{d}\bar{u}_2}{\mathrm{d}x_1} + \frac{\mathrm{d}^2\bar{u}_2}{\mathrm{d}x_1^2}\mathrm{d}x_1\right)$$
$$+V_2 \sin\frac{\mathrm{d}\bar{u}_2}{\mathrm{d}x_1} - \left(V_2 + \frac{\mathrm{d}V_2}{\mathrm{d}x_1}\mathrm{d}x_1\right)\sin\left(\frac{\mathrm{d}\bar{u}_2}{\mathrm{d}x_1} + \frac{\mathrm{d}^2\bar{u}_2}{\mathrm{d}x_1^2}\mathrm{d}x_1\right) + p_1\mathrm{d}x_1 = 0.$$

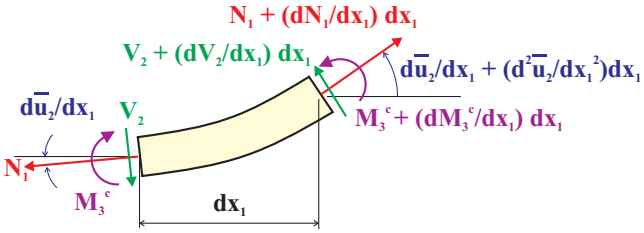

Fig. 14.6. Free body diagram of a deformed slice of the beam.

In view of assumption (14.12), $\cos(\mathrm{d}\bar{u}_2/\mathrm{d}x_1) \approx 1$, and $\sin \mathrm{d}\bar{u}_2/\mathrm{d}x_1 \approx \mathrm{d}\bar{u}_2/\mathrm{d}x_1$. Neglecting higher order differential terms in this equations, it reduces to

$$\frac{\mathrm{d}}{\mathrm{d}x_1}\left(N_1 - V_2\frac{\mathrm{d}\bar{u}_2}{\mathrm{d}x_1}\right) = -p_1.$$

Finally, assumption (14.12) implies that the second term in the parentheses is negligible as compared to the first, resulting in the following axial equilibrium equation $\mathrm{d}N_1/\mathrm{d}x_1 = -p_1$. This equation of axial force equilibrium is identical to that obtained when considering a differential element of the beam in its original, reference configuration, eq. (5.19).

The second equation of equilibrium is obtained by summing up the forces along axis $\bar{\imath}_2$ to find

$$-V_2\cos\frac{\mathrm{d}\bar{u}_2}{\mathrm{d}x_1} + \left(V_2 + \frac{\mathrm{d}V_2}{\mathrm{d}x_1}\mathrm{d}x_1\right)\cos\left(\frac{\mathrm{d}\bar{u}_2}{\mathrm{d}x_1} + \frac{\mathrm{d}^2\bar{u}_2}{\mathrm{d}x_1^2}\mathrm{d}x_1\right)$$
$$-N_1\sin\frac{\mathrm{d}\bar{u}_2}{\mathrm{d}x_1} + \left(N_1 + \frac{\mathrm{d}N_1}{\mathrm{d}x_1}\mathrm{d}x_1\right)\sin\left(\frac{\mathrm{d}\bar{u}_2}{\mathrm{d}x_1} + \frac{\mathrm{d}^2\bar{u}_2}{\mathrm{d}x_1^2}\mathrm{d}x_1\right) + p_2\mathrm{d}x_1 = 0.$$

Here again, this equation simplifies considerably when assumptions (14.12) are taken into account, leading to

$$\frac{\mathrm{d}}{\mathrm{d}x_1}\left(V_2 + N_1\frac{\mathrm{d}\bar{u}_2}{\mathrm{d}x_1}\right) = -p_2.$$

The two terms in the parentheses are now of the same order of magnitude. The equation cannot be further simplified and is recast as

$$\frac{\mathrm{d}V_2}{\mathrm{d}x_1} + \frac{\mathrm{d}}{\mathrm{d}x_1}\left(N_1\frac{\mathrm{d}\bar{u}_2}{\mathrm{d}x_1}\right) = -p_2. \tag{14.13}$$

This equilibrium equation differs from that derived earlier, eq. (5.38). The second term represents the contribution of the large axial force N_1 to the transverse equilibrium of the beam. The presence of this term stems from the fact that equilibrium conditions are expressed for a differential element of the beam in its deformed configuration.

The last equilibrium equation is obtained by summing the moments about axis $\bar{\imath}_3$ to find

$$-M_3^c + \left(M_3^c + \frac{\mathrm{d}M_3^c}{\mathrm{d}x_1}\mathrm{d}x_1 \right) + V_2 \mathrm{d}x_1 = 0. \tag{14.14}$$

After simplification this equation becomes $\mathrm{d}M_3^c/\mathrm{d}x_1 + V_2 = 0$, and is identical to that obtained earlier as eq. (5.38).

The governing equation of the problem is obtained by eliminating the shear force, V_2, from eqs. (14.13) and (5.38), then introducing the constitutive law for the bending moment, eq. (5.37), to find

$$\frac{\mathrm{d}^2}{\mathrm{d}x_1^2}\left[H_{33}^{*c} \frac{\mathrm{d}^2 \bar{u}_2}{\mathrm{d}x_1^2} \right] - \frac{\mathrm{d}}{\mathrm{d}x_1}\left[N_1 \frac{\mathrm{d}\bar{u}_2}{\mathrm{d}x_1} \right] = p_2. \tag{14.15}$$

The second term in this equation is a new term which is absent in previous developments, see eq. (5.40). The governing equation is now a fourth order differential equation for the transverse displacement field.

Four boundary conditions are required, two at each end of the beam. The boundary conditions are identical to those discussed in section 5.5.4, except when a large axial force is applied at an unsupported end of the beam. In this case, the natural boundary conditions must be derived from equilibrium of the beam in its deformed configuration. Consider, for instance, a cantilevered beam with an end tip load P_1 acting in a fixed, horizontal direction, as depicted in fig. 14.7. The boundary conditions at the tip end are

$$M_3^c = 0; \quad V_2 = -P_1 \frac{\mathrm{d}\bar{u}_2}{\mathrm{d}x_1}. \tag{14.16}$$

Governing equation (14.15) can be applied when large axial forces are present in the beam, whether in compression (N_1 is negative) or in tension (N_1 is positive). If the axial force is compressive, the beam will buckle when this compressive force reaches a critical level; if the axial force is tensile, the beam will not buckle, although its behavior will be affected by the presence of the large axial force which will tend to reduce the transverse deflection.

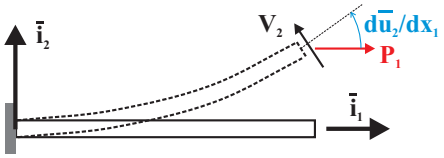

Fig. 14.7. Cantilevered beam with a tip load.

14.2.2 Buckling of a simply-supported beam (equilibrium approach)

Consider a uniform, simply-supported beam subjected to an end compressive load of magnitude P, as shown in fig. 14.5. The axial force in the beam, N_1, is constant

along its span, and $N_1 = -P$. Assuming axis $\bar{\imath}_2$ to be a principal axis of bending, the uncoupled governing equation that accounts for the presence of the large compressive load is

$$H_{33}^{*c}\frac{\mathrm{d}^4\bar{u}_2}{\mathrm{d}x_1^4} + P\frac{\mathrm{d}^2\bar{u}_2}{\mathrm{d}x_1^2} = 0. \tag{14.17}$$

with the following boundary conditions, $\bar{u}_2 = \mathrm{d}^2\bar{u}_2/\mathrm{d}x_1^2 = 0$, at the beam's root, and $\bar{u}_2 = \mathrm{d}^2\bar{u}_2/\mathrm{d}x_1^2 = 0$ at its tip. The governing equations and associated boundary conditions are homogeneous. Hence, the trivial solution, $\bar{u}_2 \equiv 0$, is a solution of the problem. The buckling load is defined as the lowest load for which a non-trivial solution of the governing equations exists.

For simplicity, the governing equation is recast in a non-dimensional form as

$$\bar{u}_2'''' + \lambda^2\bar{u}_2'' = 0, \tag{14.18}$$

where

$$\lambda^2 = \frac{PL^2}{H_{33}^{*c}}, \tag{14.19}$$

is a non-dimensional loading parameter, and $(\cdot)'$ denotes a derivative with respect to the non-dimensional span-wise variable $\eta = x_1/L$. The boundary conditions at the beam's root are $\bar{u}_2 = \bar{u}_2'' = 0$ and at its tip, $\bar{u}_2 = \bar{u}_2'' = 0$.

The solution of eq. (14.18) is

$$\bar{u}_2 = A + B\eta + C\cos\lambda\eta + D\sin\lambda\eta, \tag{14.20}$$

where A, B, C, and D, are four integration constants to be determined from the boundary conditions. The two root boundary conditions imply $A+C = 0$ and $\lambda^2 C = 0$, which in turn, implies $A = C = 0$. The solution now reduces to $\bar{u}_2 = B\eta + D\sin\lambda\eta$. The two tip boundary conditions yield

$$\begin{bmatrix} 1 & \sin\lambda \\ 0 & \sin\lambda \end{bmatrix} \begin{Bmatrix} B \\ D \end{Bmatrix} = 0. \tag{14.21}$$

This is a set of algebraic equations for the last two integration constants, B and D. Since the system is homogeneous, the solution is $B = D = 0$, which corresponds to the trivial solution of the problem. A linear system of homogeneous algebraic equations admits a non-trivial solution if and only if the determinant of the system vanishes, *i.e.*, when

$$\det\begin{bmatrix} 1 & \sin\lambda \\ 0 & \sin\lambda \end{bmatrix} = 0. \tag{14.22}$$

Expanding this determinant yield the *buckling equation*

$$\sin\lambda = 0. \tag{14.23}$$

The governing equation of the problem admits non-trivial solutions for the discrete values, λ_n, which satisfy eq. (14.23), and the lowest solution is the buckling

load. The roots of eq. (14.23) are $\lambda_n = n\pi,\ n = 1, 2, ...\infty$, which, in view of eq. (14.19), can be written as

$$(P_{\rm cr})_n = \frac{n^2\pi^2 H_{33}^{*c}}{L^2}; \quad n = 1, 2, ...\infty. \tag{14.24}$$

The lowest root corresponds to $n = 1$, resulting in a buckling load

$$P_{\rm cr} = \frac{\pi^2 H_{33}^{*c}}{L^2}. \tag{14.25}$$

The deflected shape of the beam can also be determined from this analysis. The first equation in (14.21) is $BL + D\sin\lambda = 0$, which, in view of eq. (14.23), yields $B = 0$. The deflected shape is then $\bar{u}_2 = D\sin\lambda_n\eta$. The *buckling mode shape* corresponding to the lowest buckling load is now

$$\bar{u}_2 = D\sin\pi\eta. \tag{14.26}$$

When the beam is loaded, its transverse displacement remains zero until $P = P_{\rm cr}$, at which point it buckles with the transverse deflection assuming the sinusoidal shape given by eq. (14.26). The integration constant, D, remains undetermined, *i.e.*, the transverse displacement is of arbitrary amplitude, indicating a lateral collapse of the beam. This is the same fundamental behavior presented by the rigid bar examined in section 14.1, and the unknown deflection amplitude is a direct result of the inherent linearization in the governing differential equation, eq. (14.15). A more precise description of the behavior of the structure at and beyond buckling cannot be determined within the framework of this linearized theory.

The above analysis is based on the uncoupled governing equation (14.17) pertaining to bending in plane $(\bar{\imath}_1, \bar{\imath}_2)$. A buckling analysis using the uncoupled governing equation in plane $(\bar{\imath}_1, \bar{\imath}_3)$ could be performed in the same manner, leading to the following buckling load

$$P_{\rm cr} = \frac{\pi^2 H_{22}^{*c}}{L^2}, \tag{14.27}$$

assuming, of course that the boundary conditions in planes $(\bar{\imath}_1, \bar{\imath}_2)$ and $(\bar{\imath}_1, \bar{\imath}_3)$ are identical. For the case at hand, this would mean that the beam is pinned in both directions by a ball-and-socket joint. In such cases, the buckling load is based on the lowest principal bending stiffness, and the buckling load, called the *Euler buckling load* is

$$P_{\rm Euler} = \frac{\pi^2 H^{*c}}{L^2}, \tag{14.28}$$

where H^{*c} is the lowest principal centroidal bending stiffness. This buckling load is proportional to this lowest principal centroidal bending stiffness, and inversely proportional to the square of the beam length.

14.2.3 Buckling of a simply-supported beam (imperfection approach)

In the previous section, a *perfect system* is analyzed. The beam is perfectly uniform and straight, and the line of action of the load passes exactly through the centroid. In

practical situations, no system is ever perfect: manufacturing imperfections always result in non-uniform beams, and no experimental set-up can apply a compressive load exactly at the centroid. Imperfections are always present, although their exact nature and magnitude are generally unknown.

To investigate the effect of these imperfections, a pinned-pinned beam with eccentrically applied end compressive loads will be analyzed. Figure 14.8 depicts the geometry of the problem, and it shows the compressive loads are applied at a distance e from the centroid. The governing equation of the problem is eq. (14.17) once more. The boundary conditions at the beam's root now become $\bar{u}_2 = 0$, $H_{33}^{*c}\mathrm{d}^2\bar{u}_2/\mathrm{d}x_1^2 = -Pe$ and at its tip, $\bar{u}_2 = 0$, $H_{33}^{*c}\mathrm{d}^2\bar{u}_2/\mathrm{d}x_1^2 = -Pe$.

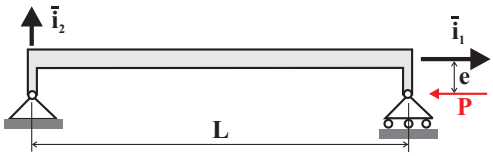

Fig. 14.8. Pinned-pinned beam with eccentric end loads.

The present problem is no longer homogeneous, because non-zero right-hand side terms appear in the boundary conditions. The trivial solution, $\bar{u}_2(x_1) \equiv 0$, is not a solution of the problem. Introducing once more the non-dimensional span and loading variables, η and λ, respectively, the differential equation can be written as eq. (14.18). The beam's root boundary conditions now become $\bar{u}_2 = 0$, $\bar{u}_2'' = -\lambda^2 e$ and at its tip, $\bar{u}_2 = 0$, $\bar{u}_2'' = -\lambda^2 e$.

The solution of eq. (14.18) is once more given by eq. (14.20). The root boundary conditions imply $A + C = 0$ and $-\lambda^2 C = -\lambda^2 e$, which yields $-A = C = e$. Proceeding with the tip boundary conditions yields $B + D\sin\lambda = e(1 - \cos\lambda$ and $-\lambda^2 D\sin\lambda = -e\lambda^2(1 - \cos\lambda)$. Solving for the last two integration constants gives $D = e(1 - \cos\lambda)/\sin\lambda$ and $B = 0$. The final solution for the transverse displacement then becomes

$$\bar{u}_2 = e\left[\frac{1-\cos\lambda}{\sin\lambda}\sin\lambda\eta + \cos\lambda\eta - 1\right] = e\left[\frac{\cos\lambda(\eta - 1/2)}{\cos\lambda/2} - 1\right]. \qquad (14.29)$$

The buckling load for the structure can be defined as the load for which the response of an initially imperfect structure becomes unbounded. Clearly, $\bar{u}_2 \to \infty$ when $\cos\lambda/2 \to 0$, *i.e.*, when $\lambda = (2n-1)\pi,\ n = 1, 2, ...\infty$. Using eq. (14.19), the dimensional buckling load now becomes

$$(P_{\mathrm{cr}})_n = \frac{(2n-1)^2\pi^2 H_{33}^{*c}}{L^2}; \quad n = 1, 2, \ldots \infty. \qquad (14.30)$$

The lowest buckling load corresponds to $n = 1$, leading to the same result given for the perfect beam in eq. (14.25). The solutions for the perfect and imperfect simply supported beams give the same buckling load.

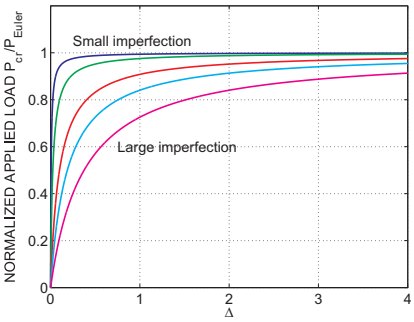

Fig. 14.9. Mid-span transverse deflection of an imperfect pinned-pinned beam for various levels of imperfection.

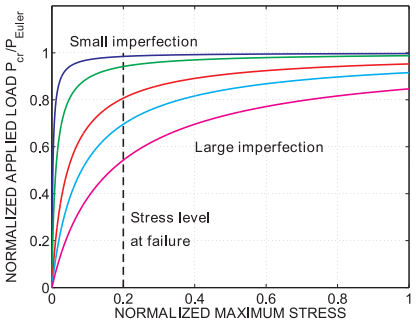

Fig. 14.10. Maximum stress in an imperfect pinned-pinned beam versus applied compressive load.

Insight into the behavior of imperfect structures can be gained by computing the mid-span deflection, Δ, of the beam. With $\eta = 1/2$, eq. (14.29) becomes

$$\Delta = \bar{u}_2\left(\eta = \frac{1}{2}\right) = e\left(\frac{1}{\cos\lambda/2} - 1\right)$$

The non-dimensional loading parameter is expressed in terms of the applied compressive load with the help of eqs. (14.19) and (14.28)

$$\lambda = \left(\frac{PL^2}{H^{*c}}\right)^{1/2} = \left(\frac{\pi^2 P}{P_{\text{Euler}}}\right)^{1/2} = \pi\left(\frac{P}{P_{\text{Euler}}}\right)^{1/2}. \tag{14.31}$$

The non-dimensional mid-span transverse deflection now becomes

$$\frac{\Delta}{e} = \frac{1}{\cos\left(\frac{\pi}{2}\sqrt{P/P_{\text{Euler}}}\right)} - 1 = \sec\left[\cos\left(\frac{\pi}{2}\sqrt{P/P_{\text{Euler}}}\right)\right] - 1. \tag{14.32}$$

Figure 14.9 depicts the mid-span deflection as a function of the applied compressive load, P, for various levels of the initial imperfection e. For all levels of imperfection, the mid-span deflection grows to infinity as the applied load approaches the buckling load. Although large mid-span deflections can occur for applied load levels far smaller than the buckling load when large imperfections are present, the buckling load itself is unaffected by the presence of imperfections.

The bending moment distribution in the beam is obtained from the transverse displacement field, eq. (14.29), as

$$M_3^c = H_{33}^{*c}\frac{\mathrm{d}^2\bar{u}_2}{\mathrm{d}x_1^2} = Pe\frac{\cos\lambda(\eta - \frac{1}{2})}{\cos\lambda/2}. \tag{14.33}$$

The maximum bending moment occurs in the middle of the beam and is $M_{\max} = Pe/\cos(\lambda/2)$. Considering a beam with a rectangular cross-section of height, h,

made of a homogeneous material with a modulus of elasticity, E, the corresponding maximum axial (compressive) stress in the beam is the sum of the uniform stress due to the axial force and of that arising from the bending moment,

$$|\sigma_{\max}| = \frac{P}{\mathcal{A}} + E\frac{M_{\max}h/2}{H_{33}^{*c}} = \frac{P}{\mathcal{A}}\left[1 + \frac{1}{2}\frac{e}{h}\frac{Sh^2}{H_{33}^{*c}}\sec\left(\frac{\pi}{2}\sqrt{\frac{P}{P_{\text{Euler}}}}\right)\right], \quad (14.34)$$

where Sh^2/H_{33}^{*c} is a non-dimensional ratio of the axial to bending stiffnesses, and e/h a measure of the imperfection's magnitude.

The beam deflects until the maximum axial stress reaches the allowable stress level, σ_{allow},

$$\frac{\sigma_{\text{allow}}\mathcal{A}}{P_{\text{Euler}}} = \frac{P_{\text{allow}}}{P_{\text{Euler}}}\left[1 + \frac{1}{2}\frac{e}{h}\frac{Sh^2}{H_{33}^{*c}}\sec\left(\frac{\pi}{2}\sqrt{\frac{P_{\text{allow}}}{P_{\text{Euler}}}}\right)\right]. \quad (14.35)$$

This is a transcendental equation for $P_{\text{allow}}/P_{\text{Euler}}$ and must be solved numerically. For structures with large imperfections, the allowable load, P_{allow}, can be substantially lower than the buckling load, P_{Euler}, as depicted in fig. 14.10.

14.2.4 Work done by the axial force

The analysis of the buckling behavior of simply-supported beams is developed in the previous section as the solution of a differential equation. The buckling load is a solution of the buckling equation, eq. (14.23), which is, in general, a transcendental equation. In view of the difficulties associated with this solution process, an alternative approach, such as an energy approach, is desirable. General procedures for obtaining approximate predictions of the static deflection of beams under transverse loading are developed in chapter 11, based on the principle of virtual work and the principle of minimum total potential energy. The latter approach requires the evaluation of the strain energy stored in the elastic system and of the work done by the externally applied forces.

Consider the problem of a cantilevered beam subjected to an axial force. When dealing with buckling problems, the strain energy stored in the deformed beam is a function of the sole curvature, as given by eq. (10.39). The work done by the axial force that causes buckling is a key aspect of the problem.

Figure 14.11 shows a differential element of the beam subjected to an axial force, N_1. In the deformed, buckled configuration of the beam, the point of application of the axial force displaces an amount δ along the line of action of the force.
Consequently, the work, $\mathrm{d}W$, done by the axial force is $\mathrm{d}W = -N_1\delta$; the minus sign reflects the fact that displacement δ occurs in the direction opposite to that of the force. Figure 14.11 indicates that $a + \delta = \mathrm{d}x_1$. Because the bending and axial loading problems are assumed to be decoupled, it follows that when undergoing bending deformation, the length of the beam remains unchanged. If the differential beam element is inextensible, $a = \mathrm{d}x_1\cos(\mathrm{d}\bar{u}_2/\mathrm{d}x_1)$, and hence,

$$\delta = \mathrm{d}x_1 - \mathrm{d}x_1 \cos\frac{\mathrm{d}\bar{u}_2}{\mathrm{d}x_1} = \mathrm{d}x_1 - \mathrm{d}x_1\left[1 - \frac{1}{2}\left(\frac{\mathrm{d}\bar{u}_2}{\mathrm{d}x_1}\right)^2 + \ldots\right], \tag{14.36}$$

where the second equality results from a Taylor series expansion of the cosine function. If the slope of the beam is assumed to remain much smaller than unity, see eq. (14.12), the higher order terms in the expansion can be neglected and $\delta = 1/2\ (\mathrm{d}\bar{u}_2\mathrm{d}x_1)^2\,\mathrm{d}x_1$. The total work done by the *internal axial forces* is then found by integration along the span of the beam

$$\Phi = \frac{1}{2}\int_0^L N_1(x_1)\left(\frac{\mathrm{d}\bar{u}_2}{\mathrm{d}x_1}\right)^2 \mathrm{d}x_1. \tag{14.37}$$

The total potential energy of the structure now becomes

$$\Pi = \frac{1}{2}\int_0^L H_{33}^{*c}\left(\frac{\mathrm{d}^2\bar{u}_2}{\mathrm{d}x_1^2}\right)^2 \mathrm{d}x_1 + \frac{1}{2}\int_0^L N_1\left(\frac{\mathrm{d}\bar{u}_2}{\mathrm{d}x_1}\right)^2 \mathrm{d}x_1 - \int_0^L p_2\,\bar{u}_2\,\mathrm{d}x_1. \tag{14.38}$$

The first term represents the strain energy associated with the bending deformation of the beam, the second the work done by the externally applied axial load, N_1, and the third the work done by the externally applied transverse load, $p_2(x_1)$.

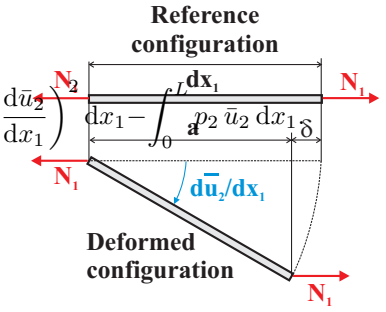

Fig. 14.11. A differential element of the beam in the deformed configuration.

The principle of minimum total potential energy requires that the total potential energy of the system is a minimum with respect to all arbitrary variations of the displacement field, and hence the total potential energy must be stationary

$$\delta\Pi = \int_0^L H_{33}^{*c}\frac{\mathrm{d}^2\bar{u}_2}{\mathrm{d}x_1^2}\,\delta\frac{\mathrm{d}^2\bar{u}_2}{\mathrm{d}x_1^2}\,\mathrm{d}x_1 + \int_0^L N_1\frac{\mathrm{d}\bar{u}_2}{\mathrm{d}x_1}\,\delta\frac{\mathrm{d}\bar{u}_2}{\mathrm{d}x_1}\,\mathrm{d}x_1 - \int_0^L p_2\,\delta\bar{u}_2\,\mathrm{d}x_1 = 0.$$

The first term is integrated by parts twice and the second once to yield

$$\int_0^L \delta\bar{u}_2\left[\frac{\mathrm{d}^2}{\mathrm{d}x_1^2}\left(H_{33}^{*c}\frac{\mathrm{d}^2\bar{u}_2}{\mathrm{d}x_1^2}\right) - \frac{\mathrm{d}}{\mathrm{d}x_1}\left(N_1\frac{\mathrm{d}\bar{u}_2}{\mathrm{d}x_1}\right) - p_2\right]\mathrm{d}x_1 + \left[H_{33}^{*c}\frac{\mathrm{d}^2\bar{u}_2}{\mathrm{d}x_1^2}\,\delta\left(\frac{\mathrm{d}\bar{u}_2}{\mathrm{d}x_1}\right)\right]_0^L + \left\{\left[N_1\frac{\mathrm{d}\bar{u}_2}{\mathrm{d}x_1} - \frac{\mathrm{d}}{\mathrm{d}x_1}\left(H_{33}^{*c}\frac{\mathrm{d}^2\bar{u}_2}{\mathrm{d}x_1^2}\right)\right]\delta\bar{u}_2\right\}_0^L = 0.$$

This equation is satisfied for arbitrary variations, $\delta\bar{u}_2(x_1)$, only if the integral and each of the boundary terms vanishes independently. The integral term vanishes if the integrand in brackets vanishes leading to the Euler-Lagrange equation of the problem,

$$\frac{\mathrm{d}^2}{\mathrm{d}x_1^2}\left(H_{33}^{*c}\frac{\mathrm{d}^2\bar{u}_2}{\mathrm{d}x_1^2}\right) - \frac{\mathrm{d}}{\mathrm{d}x_1}\left(N_1\frac{\mathrm{d}\bar{u}_2}{\mathrm{d}x_1}\right) = p_2.$$

This is the governing differential equation of the problem. It is identical to eq. (14.15) that is obtained from the equilibrium conditions for a differential element of the beam in the deformed configuration, see section 14.2.2.

For a cantilevered beam, the geometric boundary conditions at the beam's root imply $\bar{u}_2 = 0$ and $\mathrm{d}\bar{u}_2/\mathrm{d}x_1 = 0$. Because the variations at the beam's tip, $\delta(\mathrm{d}\bar{u}_2(L)/\mathrm{d}x_1)$ and $\delta\bar{u}_2(L)$, are arbitrary, $H_{33}^{*c}\mathrm{d}^2\bar{u}_2(L)/\mathrm{d}x_1^2 = 0$ and $N_1\mathrm{d}\bar{u}_2(L)/\mathrm{d}x_1 - \mathrm{d}/\mathrm{d}x_1(H_{33}^{*c}\mathrm{d}^2\bar{u}_2/\mathrm{d}x_1^2) = 0$, respectively. The first condition corresponds to the vanishing of the bending moment at the tip of the beam, as expected; the second condition corresponds to $N_1\,\mathrm{d}\bar{u}_2(L)/\mathrm{d}x_1 + V_2(L) = 0$. These boundary conditions are identical to those derived in section 14.2.2, see eq. (14.16), and correspond to the tip equilibrium equations of the beam in its deformed configuration.

The energy approach developed in this section leads to the same governing differential equation and boundary conditions obtained from the equilibrium approach in section 14.2.1. This result should be expected because the principle of minimum total potential energy is derived from the equations of equilibrium.

14.2.5 Buckling of a simply-supported beam (energy approach)

Consider a uniform, simply-supported beam of length L subjected to an end compressive load of magnitude P, as depicted in fig. 14.5. The beam is assumed to be pinned about axis $\bar{\imath}_3$ which is perpendicular to the plane of symmetry of the beam. The axial force in the beam, N_1, is constant along the span, and $N_1 = -P$. The total potential energy of the system, eq. (14.38), becomes

$$\mathit{\Pi} = \frac{1}{2}\int_0^L H_{33}^{*c}\left(\frac{\mathrm{d}^2\bar{u}_2}{\mathrm{d}x_1^2}\right)^2 \mathrm{d}x_1 - \frac{1}{2}\int_0^L P\left(\frac{\mathrm{d}\bar{u}_2}{\mathrm{d}x_1}\right)^2 \mathrm{d}x_1.$$

An approximate solution can be developed by expressing $\bar{u}_2(x_1)$ as a sum of shape functions, each of which satisfies the geometric boundary conditions, see section 11.4.

Solution using a single shape function

The geometric boundary conditions for a simply supported beam require the displacement to vanish at both end. An assumed transverse displacement field that satisfies these conditions is

$$\bar{u}_2(x_1) = q_j \sin\frac{j\pi x_1}{L} \tag{14.39}$$

where q_j is the single degree of freedom of the problem and j an unspecified integer.

Substituting this assumed displacement field into the expression for the total potential energy, eq. (14.38), and carrying out the integrations yields the total potential energy as a function of the degree of freedom

$$\mathit{\Pi} = \left[H_{33}^{c}\left(\frac{j\pi}{L}\right)^2 - P\right]\left(\frac{j\pi}{L}\right)^2 \frac{L}{2}\,q_j^2.$$

The principle of minimum total potential energy requires the total potential energy to be a minimum with respect to the choice of the degrees of freedom, leading to

$$\frac{\partial \Pi}{\partial q_j} = \left[H_{33}^c \left(\frac{j\pi}{L} \right)^2 - P \right] \left(\frac{j\pi}{L} \right)^2 L q_j = 0.$$

This homogeneous equation admits a trivial solution, $q_j = 0$, which implies $\bar{u}_2(x_1) \equiv 0$. A nontrivial solution exists if $(j^2\pi^2 H_{33}^c/L^2 - P) = 0$, and this condition yields the critical load,

$$P_{\text{cr}} = j^2\pi^2 \frac{H_{33}^c}{L^2}.$$

The lowest critical load is obtained when $j = 1$ and defines the buckling load, $P_{\text{cr}} = \pi^2 H_{33}^c/L^2$. The buckling shape is given by eq. (14.39) as $\bar{u}_2(x_1) = q_1 \sin(\pi x_1)/L^2$.

This result is identical to that obtained in section 14.2.2. This should not be surprising because the shape function given in eq. (14.39) is, in fact, the exact solution. An infinite number of critical loads are obtained for all values of integer j, but the lowest critical load is the buckling load.

Solution using multiple shape functions

The following transverse displacement field containing two shape functions will be assumed next

$$\bar{u}_2(x_1) = q_1 h_1(x_1) + q_2 h_2(x_1) = q_1 \sin \frac{\pi x_1}{L} + q_2 \sin \frac{2\pi x_1}{L} = \underline{H}^T(x_1)\underline{q}, \quad (14.40)$$

where h_1 and h_2 are the assumed shape functions, $\underline{H}$ the displacement interpolation array defined by eq. (11.62), and $\underline{q} = \{q_1, q_2\}^T$ the solution array. In this case, the shape functions are selected as sine functions. In general, N shape functions could be used, but the assumed shape functions must all satisfy the geometric boundary conditions of the problem.

Calculation of the integrals in eq. (14.38) requires the first and second derivatives of the transverse deflection which can be expressed in matrix form as follows

$$\frac{\mathrm{d}\bar{u}_2}{\mathrm{d}x_1} = q_1 \frac{\pi}{L} \cos \frac{\pi x_1}{L} + q_2 \frac{2\pi}{L} \cos \frac{2\pi x_1}{L} = \underline{G}^T(x_1)\underline{q}, \quad (14.41a)$$

$$\frac{\mathrm{d}^2\bar{u}_2}{\mathrm{d}x_1^2} = -q_1 \left(\frac{\pi}{L} \right)^2 \sin \frac{\pi x_1}{L} - q_2 \left(\frac{2\pi}{L} \right)^2 \sin \frac{2\pi x_1}{L} = \underline{B}^T(x_1)\underline{q}. \quad (14.41b)$$

The *displacement gradient interpolation array*, $\underline{G}(x_1)$, is defined as

$$\underline{G}(x_1) = \left\{ \frac{\mathrm{d}h_1}{\mathrm{d}x_1}, \frac{\mathrm{d}h_2}{\mathrm{d}x_1}, \ldots \frac{\mathrm{d}h_N}{\mathrm{d}x_1} \right\}^T, \quad (14.42)$$

and the *curvature interpolation array*, $\underline{B}(x_1)$, is given by eq. (11.72).

The strain energy in the structure is readily evaluated using the general procedure described in section 11.4.3. The strain energy is expressed as $A = 1/2\ \underline{q}^T \underline{\underline{K}}\, \underline{q}$, see eq. (11.75). The stiffness matrix is given by eq. (11.67) as

$$\underline{\underline{K}} = \int_0^L \underline{B}(x_1)\, H_{33}^c(x_1) \underline{B}^T(x_1)\, \mathrm{d}x_1. \tag{14.43}$$

For the shape functions defined in eq. (14.40), the stiffness matrix becomes

$$\underline{\underline{K}} = \frac{\pi^4 H_{33}^c}{2L^3} \begin{bmatrix} 1 & 0 \\ 0 & 16 \end{bmatrix}. \tag{14.44}$$

The second integral in eq. (14.38) represent the work done by the applied axial load. Using eq. (14.41a), it can be evaluated as follows

$$\begin{aligned} \Phi &= -\frac{1}{2} \int_0^L P \left(\frac{\mathrm{d}\bar{u}_2}{\mathrm{d}x_1} \right)^2 \mathrm{d}x_1 = -\frac{P}{2} \int_0^L \left(\underline{G}^T \underline{q} \right)^T \left(\underline{G}^T \underline{q} \right) \mathrm{d}x_1 \\ &= \frac{1}{2} \underline{q}^T P \left[\int_0^L \underline{G}\, \underline{G}^T \, \mathrm{d}x_1 \right] \underline{q} = \frac{1}{2} \underline{q}^T P \underline{\underline{K}}_G\, \underline{q}, \end{aligned}$$

where the *geometric stiffness matrix*, $\underline{\underline{K}}_G$, is defined as

$$\underline{\underline{K}}_G = \int_0^L \underline{G}(x_1) \underline{G}^T(x_1)\, \mathrm{d}x_1. \tag{14.45}$$

For the problem at hand, this matrix is

$$\underline{\underline{K}}_G = \frac{\pi^2}{2L} \begin{bmatrix} 1 & 0 \\ 0 & 4 \end{bmatrix}. \tag{14.46}$$

The total potential energy of the structure is now found by combining the strain energy and the work done by the axial force as

$$\Pi = \frac{1}{2}\, \underline{q}^T \underline{\underline{K}}\, \underline{q} - \frac{1}{2}\, \underline{q}^T P \underline{\underline{K}}_G\, \underline{q} = \frac{1}{2}\, \underline{q}^T \left[\underline{\underline{K}} + P \underline{\underline{K}}_G \right] \underline{q}.$$

This is a positive-definite quadratic form in $\underline{q}$, and from the principle of minimum total potential energy, it must assume a minimum when the system is in equilibrium. It is shown in appendix A.2.9 that this quadratic form is minimum when the solution array, $\underline{q}$, satisfies the following condition

$$\left[\underline{\underline{K}} + P \underline{\underline{K}}_G \right] \underline{q} = 0. \tag{14.47}$$

This is a set of homogeneous, algebraic equations for the solution array, $\underline{q}$; the solution of this homogeneous system is the trivial solution, $\underline{q} = 0$, which corresponds to the vanishing of the transverse displacement field.

In the equilibrium approach developed in section 14.2.5, a trivial solution is also found. The buckling load of the system is defined as the lowest load for which a non-trivial solution of the governing equations exists. A nontrivial solution of the homogeneous, algebraic system given by eq. (14.47) exists if and only if the determinant of the system vanishes,

$$\det\left(\underline{\underline{K}} - P\underline{\underline{K}}_G\right) = 0. \tag{14.48}$$

This is the *buckling equation* for the system, and the values of the axial compressive load, P, for which this determinant vanishes are the critical loads. Introducing the stiffness matrix, eq. (14.44), and the geometric stiffness matrix, eq. (14.46), leads to an explicit expression for the buckling equation

$$\det\left\{\frac{\pi^2}{2L}\begin{bmatrix}\dfrac{\pi^2 H_{33}^{*c}}{L^2} - P & 0 \\ 0 & 16\dfrac{\pi^2 H_{33}^{*c}}{L^2} - 4P\end{bmatrix}\right\} = 0. \tag{14.49}$$

The solutions of this buckling equation are $P = \pi^2 H_{33}^{*c}/L^2$ and $4\pi^2 H_{33}^{*c}/L^2$. The lowest solution is the buckling load $P_{\text{cr}} = \pi^2 H_{33}^{*c}/L^2$. This buckling load is identical to that found from the equilibrium approach, see section 14.2.5. Again, this should be expected because the exact buckling mode shape, $\sin \pi x_1/L$, see eq. (14.26), is one of the assumed mode shapes in eq. (14.40).

The solutions of the buckling equation give rise to non-trivial solutions of the problem. Since the stiffness and geometric stiffness matrices are, in general, matrices of size $N \times N$, the expansion of the determinant equation leads to an N^{th} order algebraic equation in P, and hence, solutions P_i, $i = 1, 2, \ldots, N$. For large values of N, the coefficients of this algebraic equation become very large, and the solution process becomes increasingly difficult, leading to inaccurate solutions. In this case, it is preferable to recast eq. (14.48) as $\underline{\underline{K}}\,\underline{q} = P\underline{\underline{K}}_G\,\underline{q}$. Multiplying through by $\underline{\underline{K}}^{-1}$ then yields

$$\underline{\underline{D}}\,\underline{q} = \lambda\,\underline{q}, \tag{14.50}$$

where $\underline{\underline{D}} = \underline{\underline{K}}^{-1}\underline{\underline{K}}_G$ and $\lambda = 1/P$. This is an eigenvalue problem of the type described in appendix A.2.4, and the eigenvalues, λ, are the reciprocals of the critical loads.

Matrix $\underline{\underline{D}}$ is of size $N \times N$ and it possesses N eigenvalues λ_i, $i = 1, 2, \cdots, N$, see appendix A.2.4. Let λ_1 be the highest eigenvalue of $\underline{\underline{D}}$; $P_{\text{cr}} = 1/\lambda_1$ is then an approximation to the lowest critical load of the system, which is the buckling load. If $\underline{q}_1$ is the corresponding eigenvector, the buckling mode shape is $\bar{u}_2(x_1) = \underline{H}^T(x_1)\,\underline{q}_1$.

The procedure described in this section can be summarized by the following steps.

1. Select N shape functions that satisfy the geometric boundary conditions. Construct the corresponding displacement, displacement gradient, and strain interpolation arrays.

2. Compute the strain energy of the structure, leading to the $N \times N$ stiffness matrix, $\underline{\underline{K}}$, see eq. (14.43).
3. Compute the work done by the axial forces, leading to the $N \times N$ geometric stiffness matrix, $\underline{\underline{K}}_G$, see eq. (14.45).
4. Solve the eigenproblem $\underline{\underline{D}}\,\underline{q} = \lambda \underline{q}$, where $\underline{\underline{D}} = \underline{\underline{K}}^{-1}\underline{\underline{K}}_G$, to find the highest eigenvalue λ_1, and corresponding eigenvector $\underline{q}_1$.
5. The approximate buckling load of the structure is $P_{\text{cr}} = 1/\lambda_1$ and the buckling mode shapes is $\bar{u}_2(x_1) = \underline{H}^T(x_1)\underline{q}_1$.

If externally applied transverse loads are also applied, the above procedure must be modified as follows.

1. Select N shape functions that satisfy the geometric boundary conditions. Construct the corresponding displacement, displacement gradient, and strain interpolation arrays.
2. Compute the strain energy of the structure, leading to the $N \times N$ stiffness matrix, $\underline{\underline{K}}$.
3. Compute the work done by the externally applied transverse loads, leading to the load array, $\underline{Q}$.
4. Compute the work done by the axial forces, leading to the $N \times N$ geometric stiffness matrix, $\underline{\underline{K}}_G$.
5. Solve the linear system $(\underline{\underline{K}} - P\underline{\underline{K}}_G)\underline{q} = \underline{Q}$ to find the solution array, $\underline{q}$.

In this case, the solution procedure assumes that matrix $(\underline{\underline{K}} - P\underline{\underline{K}}_G)$ is non-singular, *i.e.*, $\det(\underline{\underline{K}} - P\underline{\underline{K}}_G) \neq 0$. If the axial force is such that $\det(\underline{\underline{K}} - P\underline{\underline{K}}_G) = 0$, the linear system cannot be solved, and P has reached the buckling load.

14.2.6 Applications to beam buckling

A number of examples will be worked to illustrate the use of both the equilibrium and energy approaches.

Example 14.1. Cantilevered beam with tip support (equilibrium approach)
Consider a uniform, cantilevered beam with a tip support as depicted in fig. 14.12. The beam is subjected to an axial compressive load P at the tip. The resulting axial force in the beam, N_1, is constant along the span, and $N_1 = -P$. The governing differential equation of the problem is given by eq. (14.17), with the following boundary conditions at the beam's root $\bar{u}_2 = \mathrm{d}\bar{u}_2/\mathrm{d}x_1 = 0$ and at its tip $\bar{u}_2 = \mathrm{d}^2\bar{u}_2/\mathrm{d}x_1^2 = 0$. The non-dimensional span-wise variable $\eta = x_1/L$ is defined and the governing equation then reduces to eq. (14.18), where $(\cdot)'$ denotes a derivative with respect to η and the non-dimensional loading parameter, λ^2, is defined by eq. (14.19). The boundary conditions at the beam's root become $\bar{u}_2 = \bar{u}_2' = 0$ and at its tip $\bar{u}_2 = \bar{u}_2'' = 0$.

The solution of eq. (14.18) is

$$\bar{u}_2 = A + B\eta + C\cos\lambda\eta + D\sin\lambda\eta$$

where A, B, C, and D, are four integration constants to be determined from the boundary conditions. The first two boundary conditions imply $A + C = 0$ and $B +$

$\lambda D = 0$. Eliminating constants B and C yields $\bar{u}_2 = A(1-\cos\lambda\eta)+D(\sin\lambda\eta-\lambda\eta)$. The last two boundary conditions then yield

$$\begin{bmatrix} 1-\cos\lambda & \sin\lambda-\lambda \\ \cos\lambda & -\sin\lambda \end{bmatrix} \begin{Bmatrix} A \\ D \end{Bmatrix} = 0.$$

Fig. 14.12. Cantilevered beam with tip support under axial load.

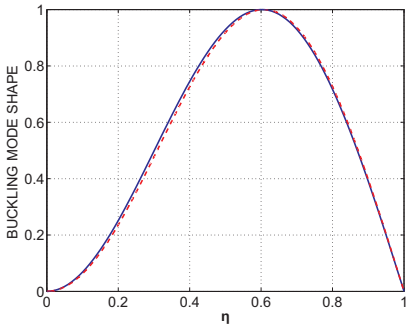

Fig. 14.13. Buckling mode shape for the cantilevered beam with tip support. Exact solution: solid line; approximate solution ($n = 1$): dashed line.

This is a set of algebraic equations for the last two integration constants, A and D. Because the system is homogeneous, the solution is $A = D = 0$, which corresponds to the trivial, non-buckled, solution of the problem. A linear system of homogeneous algebraic equations admits a non-trivial solution if and only if the determinant of the system vanishes,

$$\det \begin{bmatrix} 1-\cos\lambda & \sin\lambda-\lambda \\ \cos\lambda & -\sin\lambda \end{bmatrix} = 0.$$

Expanding this determinant yield the *buckling equation*, $\tan\lambda-\lambda = 0$. The buckling equation is a transcendental equation, and the lowest solution is $\lambda = 4.4934$. The buckling load of the system is $P_{\rm cr} = (4.4934)^2 H_{33}^{*c}/L^2$. For comparison, this can be recast as $P_{\rm cr} = 2.0457\pi^2 H_{33}^{*c}/L^2 = 2.0457 P_{\rm Euler}$, or about twice the buckling load for a simply supported beam of the same length.

The buckling mode shape can be determined from this analysis. The buckling equation implies $A\cos\lambda = D\sin\lambda$ or $A = D\tan\lambda = \lambda D$. the buckling mode shape is then $\bar{u}_2(\eta) = D\,[\lambda(1-\eta)+\sin\lambda\eta-\lambda\cos\lambda\eta]$. The integration constant, D, remains undetermined, which means that the transverse displacement is of arbitrary amplitude, indicating a lateral collapse of the beam.

Example 14.2. Cantilevered beam with tip support (energy approach)
Consider the same cantilevered beam with a tip support depicted in fig. 14.12. An energy approach will be used to find an approximate solution to the problem. The following transverse displacement field will be assumed

$$\bar{u}_2(x_1) = \sum_{n=1}^{N} q_n \, h_n(\eta) = \sum_{n=1}^{N} q_n \, \frac{1}{2} \left[\cos a_n \eta - \cos b_n \eta \right], \tag{14.51}$$

where $\eta = x_1/L$ is the non-dimensional span-wise variable, $a_n = (n - 1/2)\pi$ and $b_n = (n + 1/2)\pi$. Note that each assumed shape function satisfies the geometric boundary conditions of the problem: $h_n(0) = 0$, $h_n'(0) = 0$, and $h_n(1) = 0$, where $(\cdot)'$ denotes a derivative with respect to η.

The displacement field is written as $\bar{u}_2(x_1) = \underline{H}^T(\eta)\, \underline{q}$, where $\underline{H}$ is the displacement interpolation array, and $\underline{q}^T$ the solution array. The displacement gradient and the curvature interpolation arrays are given by eqs. (14.41) as

$$\frac{\mathrm{d}\bar{u}_2}{\mathrm{d}x_1} = \sum_{n=1}^{N} \frac{q_n}{2L} \left[-a_n \sin a_n \eta + b_n \sin b_n \eta \right] = \underline{G}^T(\eta)\, \underline{q},$$

$$\frac{\mathrm{d}^2\bar{u}_2}{\mathrm{d}x_1^2} = \sum_{n=1}^{N} \frac{q_n}{2L^2} \left[-a_n^2 \cos a_n \eta + b_n^2 \cos b_n \eta \right] = \underline{B}^T(\eta)\, \underline{q}.$$

The bending and geometric stiffness matrices are computed using eqs. (14.43) and (14.45), and using the first four terms in eq. (14.51) results in

$$\underline{\underline{K}} = \frac{H_{33}^{*c}}{4L^3} \left(\frac{\pi}{2} \right)^4 \begin{bmatrix} 1^4 + 3^4 & -3^4 & 0 & 0 \\ -3^4 & 3^4 + 5^4 & -5^4 & 0 \\ 0 & -5^4 & 5^4 + 7^4 & -7^4 \\ 0 & 0 & -7^4 & 7^4 + 9^4 \end{bmatrix},$$

and

$$\underline{\underline{K}}_G = \frac{1}{4L} \left(\frac{\pi}{2} \right)^2 \begin{bmatrix} 1^2 + 3^2 & -3^2 & 0 & 0 \\ -3^2 & 3^2 + 5^2 & -5^2 & 0 \\ 0 & -5^2 & 5^2 + 7^2 & -7^2 \\ 0 & 0 & -7^2 & 7^2 + 9^2 \end{bmatrix}.$$

The buckling equation is given by eq. (14.48). If a single term is taken in the assumed displacement field, *i.e.*, if $N = 1$, the buckling load is found to be $P_{\mathrm{cr}} = 82/10(\pi/2)^2 H_{33}^{*c}/L^2 = 2.0500\pi^2 H_{33}^{*c}/L^2$. This compares very favorably with the exact solution found in the previous example as $P_{\mathrm{cr}} = 2.0457\pi^2 H_{33}^{*c}/L^2$. A two term approximation yields $P_{\mathrm{cr}} = 2.0467\pi^2 H_{33}^{*c}/L^2$ that overestimates the exact solution by 0.05% only. For larger values of N more accurate solutions are obtained, but it is the preferable to rely on the solution of the eigenproblem defined by eq. (14.50).

Figure 14.13 depicts the buckling mode shape for the exact solution developed in the previous example and the present approximate solution using a single assumed mode, *i.e.*, with $N = 1$. For $N = 2$, the exact and approximate buckling mode shapes are almost coincident.

Example 14.3. Cantilevered beam with linearly tapered depth

During buckling of a cantilevered beam, the region near the root undergoes the largest bending moment. To increase the buckling load, it is reasonable to increase the depth of the section in the root region to provide a greater bending stiffness.

To investigate this effect, consider a cantilevered beam with a depth in plane $(\bar{\imath}_2, \bar{\imath}_1)$ that is tapered linearly from h_r at the root to h_t at the tip, as shown in fig. 14.14. From a practical point of view, assume also that either the beam is restrained from deflection in the $\bar{\imath}_3$ direction or else $H^c_{22} \gg H^c_{33}$ so that buckling in plane $(\bar{\imath}_1, \bar{\imath}_3)$ will not occur.

For a beam with a rectangular cross-section having a linearly tapered depth, the bending stiffness can be written as

$$H^c_{33} = H_0 \left[\bar{h} - (\bar{h} - 1)\eta\right]^3, \tag{14.52}$$

where $\eta = x_1/L$ is a non-dimensional span-wise variable, H_0 the tip bending stiffness, and $\bar{h} = h_r/h_t > 1$ the root depth factor.

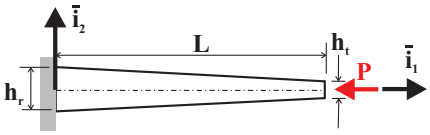

Fig. 14.14. Tapered cantilevered beam under axial load.

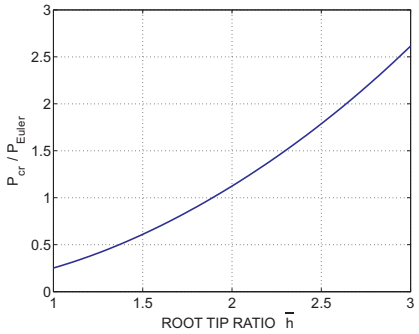

Fig. 14.15. Buckling load for tapered cantilevered beam as a function of the root depth to the tip depth, $\bar{h}$.

The following transverse displacement field satisfies the geometric boundary conditions

$$\bar{u}_2(x_1) = \sum_{n=1}^{N} q_n \, \eta^{n+1} = \sum_{n=1}^{N} q_n \, h_n(\eta), \tag{14.53}$$

where the shape functions are $h_n(\eta) = \eta^{n+1}$. For $N = 2$, the displacement gradient and curvature interpolation arrays are $\underline{G} = [2\eta,\ 3\eta^2]/L$ and $\underline{B} = [2,\ 6\eta]/L^2$, respectively.

The bending stiffness matrix, $\underline{\underline{K}}$, and geometric stiffness matrix, $\underline{\underline{K}}_G$, are found from eqs. (14.43) and (14.45), respectively, as

$$\underline{\underline{K}} = \frac{H_0}{5L^2} \begin{bmatrix} 5(1 + \bar{h} + \bar{h}^2 + \bar{h}^3) & 3(4 + 3\bar{h} + 2\bar{h}^2 + \bar{h}^3) \\ 3(4 + 3\bar{h} + 2\bar{h}^2 + \bar{h}^3) & 3(10 + 6\bar{h} + 3\bar{h}^2 + \bar{h}^3) \end{bmatrix},$$

and

$$\underline{\underline{K}}_G = \frac{1}{30L} \begin{bmatrix} 40 & 45 \\ 45 & 54 \end{bmatrix},$$

From eq. (14.50), the critical loads are the reciprocals of the two eigenvalues of the matrix $\underline{\underline{D}} = \underline{\underline{K}}^{-1}\underline{\underline{K}}_G$. The buckling load is the lowest of these. Figure 14.15 shows the increase in buckling load as the root depth factor, $\bar{h}$, increases. For $\bar{h} = 1$, the beam is a cantilever with uniform depth, and the buckling load is $P_{\rm cr} = 0.2519 P_{\rm Euler}$ where $P_{\rm Euler} = \pi^2 H^{*c}/L^2$. This compares very favorably with the exact buckling load, $P_{\rm cr} = 0.2500 P_{\rm Euler}$. For $\bar{h} = 2$, the buckling load is approximately the same as that obtained for cantilevered beam with tip support, see example 14.1. For $\bar{h} = 3.7$, the buckling load is equal to that of a uniform, simply supported beam of the identical length and tip bending stiffness.

14.2.7 Buckling of beams with various end conditions

The analysis method developed in the previous section can be repeated for beams with various end conditions. The buckling load for various configurations are summarized in table 14.1 which lists the non-dimensional buckling parameter k, such that

$$P_{\rm cr} = \bar{k}\pi^2 \frac{H^{*c}_{33}}{L^2} = \bar{k}\, P_{\rm Euler}.$$

Table 14.1. Buckling loads for beams with various end conditions.

Boundary Conditions	Buckling parameter $\bar{k}$
Clamped - Free	1/4
Clamped - Clamped	4
Clamped - Pinned	2.0457
Pinned - Pinned	1

Finally, it should be noted that in all the previous examples, it is assumed that the beam under consideration is supported in such a way that it is free to buckle in plane $(\bar{\imath}_1, \bar{\imath}_2)$. This can be assured if this is a plane of symmetry or contains one of the principal axes of bending and if the bending stiffness is the minimum for the given cross-section.

14.2.8 Problems

Problem 14.1. Uniform cantilevered beam
Consider a uniform cantilevered beam of length L subjected to an axial compressive load P. Find the lowest buckling load of the system and the associated buckling mode shape. Check your predictions with the results listed in table 14.1.

Problem 14.2. Simply-supported beam with end torsional springs
Consider a simply-supported beam with end torsional springs of stiffness k subjected to an axial compressive load P, as depicted in fig. 14.16. It will be convenient to use the non-dimensional load $P/P_{\rm Euler}$ where $P_{\rm Euler} = \pi^2 H^{*c}_{33}/L^2$ and non-dimensional spring constant $\bar{k} = kL/H^{*c}_{33}$. *(1)* Find the lowest buckling load $P_{\rm cr}$ of the system. Plot $P_{\rm cr}$ as a function of

$\bar{k}$. Discuss the limiting cases $\bar{k} = 0$ and $\bar{k} = \infty$. *(2)* Use an energy method to estimate the lowest buckling load of the system. Select the following assumed displacements $\bar{u}_2(x_1) = q_1 \sin \pi x_1/L + q_2 \sin 2\pi x_1/L$. *(3)* Plot the exact and approximate buckling loads on the same graph. Comment on the accuracy of the approximate solution. How would you improve its accuracy?

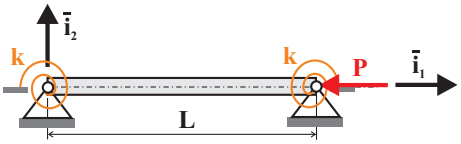

Fig. 14.16. Simply-supported beam with end torsional springs.

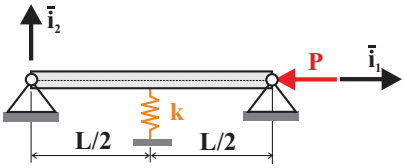

Fig. 14.17. Simply-supported beam with a mid-span spring.

Problem 14.3. Simply-supported beam with a mid-span spring

Study the effect of a mid-span spring of stiffness constant k on the buckling load of the simply-supported beam of span L depicted in fig. 14.17. To investigate this problem, use an energy approach with the following assumed mode shapes $\bar{u}_2(\eta) = q_1 \sin \pi\eta + q_2 \sin 2\pi\eta + a_3 \sin 3\pi\eta$. It is convenient to use the following notation: $P_{\text{Euler}} = \pi^2 H^{*c}_{33}/L^2$ is the Euler buckling load for the beam in the absence of the mid-span spring, $\bar{k} = kL^3/H^{*c}_{33}$ the non-dimensional stiffness of the spring, and $\eta = x_1/L$ the non-dimensional span variable. *(1)* Find the buckling loads of the system. *(2)* How does the lowest buckling load vary when $\bar{k}$ increases? Plot the non-dimensional buckling loads P/P_e as a function of $\bar{k}$. *(3)* How much improvement in buckling load can be expected from the mid-span spring.

Problem 14.4. Cantilevered beam with axial and transverse loads

Consider the cantilevered beam of length L subjected to tip axial load in tension, T, and tip transverse load, P, as depicted in fig. 14.18. *(1)* Write the governing differential equation of the problem and the associated boundary conditions. *(2)* Find the transverse displacement field of the beam.

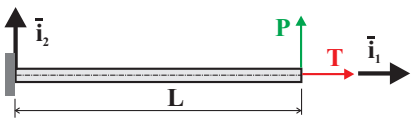

Fig. 14.18. Cantilevered beam subjected to tip axial and transverse loads.

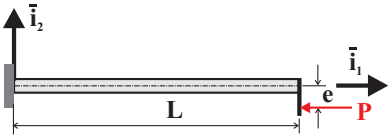

Fig. 14.19. Cantilevered beam subjected to tip axial load with an off-set.

Problem 14.5. Various short questions

Consider a cantilevered beam subjected to a tip compressive load applied with an off-set e, as depicted in fig. 14.19. Let P_{Euler} denote the Euler buckling load on the system. *(1)* For the perfect system, *i.e.*, for $e = 0$, is the buckling load of the system affected by the strength of the

material the beam is made of? *(2)* For the imperfect system, *i.e.*, for $e \neq 0$, is the buckling load of the system affected by the strength of the material the beam is made of? *(3)* For the perfect system, *i.e.*, for $e = 0$, does the beam experience transverse deflections when $P < P_{\text{Euler}}$? *(4)* For the imperfect system, *i.e.*, for $e \neq 0$, does the beam experience transverse deflections when $P < P_{\text{Euler}}$? *(5)* Consider an imperfect system, *i.e.*, $e \neq 0$, under increasing load P. Does the material allowable stress play a role in predicting the allowable applied load P? Explain your answers to all the above questions; a YES/NO answer is not valid.

Problem 14.6. Cantilevered beam with tip support

A uniform cantilevered beam of span L has a tip support, as depicted in fig. 14.20. The beam is subjected to a tip compressive axial force P and a uniform transverse loading p_0. *(1)* Find the exact solution of the problem when the beam is *subjected to the sole transverse load* p_0. *(2)* Find an approximate solution for the problem when the beam is *subjected to the combined loading*, *i.e.*, both transverse loading p_0 and tip compressive load P are applied. Use an energy method with a single assumed mode selected to be the solution to part 1. *(3)* Determine the buckling load P_{cr} for this problem. *(4)* How is the buckling load affected by the transverse loading p_0. *(5)* Under the combined loading condition, find the failure envelope in the two-dimensional space $P/P_{\text{cr}}, p_0/(b\sigma_{\text{ult}})$. Failure is reached when $|\sigma_{\text{ben}}^{\max}| + |\sigma_{\text{axi}}^{\max}| = \sigma_{\text{ult}}$, where $\sigma_{\text{ben}}^{\max}$ and $\sigma_{\text{axi}}^{\max}$ are the the maximum stresses due to bending and axial force, respectively, and σ_{ult} the ultimate allowable stress for the material. Use the following data $E = 73.0$ GPa, $\sigma_{\text{ult}} = 620$ MPa. Plot two failure envelopes for $L/h = 20$ and 10 on the same graph. Assume a rectangular section of width b and hight h.

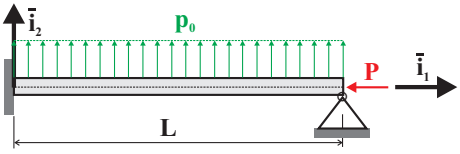

Fig. 14.20. Cantilevered beam with tip support subjected to a compressive load.

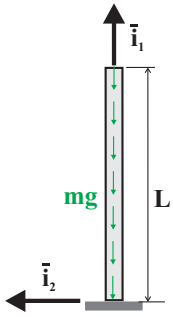

Fig. 14.21. Flag pole standing under its own weight.

Problem 14.7. Flag pole standing under its own weight

A flagpole of uniform mass per unit span m is standing up against gravity, as depicted in fig. 14.21. What is the critical weight mg_{cr} such that this flagpole will buckle under its own weight? *(1)* Use an energy method to solve this problem. Use the following assumed mode $\bar{u}_2(\eta) = a\,(1 - \cos \pi\eta/2)$. *(2)* If the flagpole is made of steel and has a square cross-section (1cm$\times$ 1cm), what is the critical length at which it will buckle under its own weight. (For steel: material density $\rho = 7700\text{kg/m}^3$, Young's modulus $E = 210$ GPa; $g = 9.81\text{m/sec}^2$).

Problem 14.8. Cantilevered beam with tip spring

An axial compressive load P is applied at the centroid of a uniform, cantilevered beam of span L with a tip spring of stiffness k, as depicted in fig. 14.22. *(1)* Derive the exact buckling equa-

tion for this problem in terms of the following non-dimensional parameters $\lambda^2 = PL^2/H_{33}^{*c}$, $\bar{k} = kL^3/H_{33}^{*c}$. *(2)* Plot the buckling load of the system for $\bar{k} \in [0, 75]$. *(3)* Find an approximate solution of the problem using an energy approach with the following assumed mode $\bar{u}_2 = q_1(\eta^4 - 4\eta^3 + 6\eta^2) + q_2(2\eta^4 - 5\eta^3 + 3\eta^2)$, where $\eta = x_1/L$. *(4)* Compare your results by plotting the exact and approximate buckling loads of the system for $\bar{k} \in [0, 75]$.

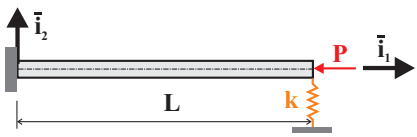

Fig. 14.22. Cantilevered beam with tip spring.

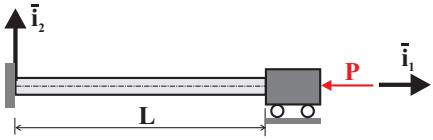

Fig. 14.23. Clamped-clamped beam under tip load.

Problem 14.9. Clamped-clamped beam under tip load

Consider the clamped-clamped beam of length L depicted in fig. 14.23. The beam is subjected to a compressive load P. *(1)* Find the lowest buckling load of this system using the differential equation approach. *(2)* Find the lowest buckling load of the system using an energy approach with the following assumed mode $\bar{u}_2(\eta) = a(\eta^2 - 2\eta^3 + \eta^4)$, where $\eta = x_1/L$ is the non-dimensional variable along the beam span.

Problem 14.10. Portal frame subjected to compressive loads

Consider the portal frame shown in fig. 14.24. Note that the problem is symmetric, and hence it is sufficient to consider one of the vertical beams with a tip torsional spring of stiffness constant k and subjected to a compressive load P. *(1)* Verify that $k = 6J_{33}/w$. *(2)* Find the lowest buckling load of the system. Show that the non-dimensional critical load depends on the non-dimensional parameter $\beta = (H_{33}w)/(J_{33}h)$. *(3)* Plot the lowest buckling load as a function of β. Discuss the meaning of your results when $\beta = 0$ and ∞.

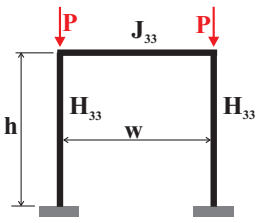

Fig. 14.24. Portal frame subjected to compressive loads.

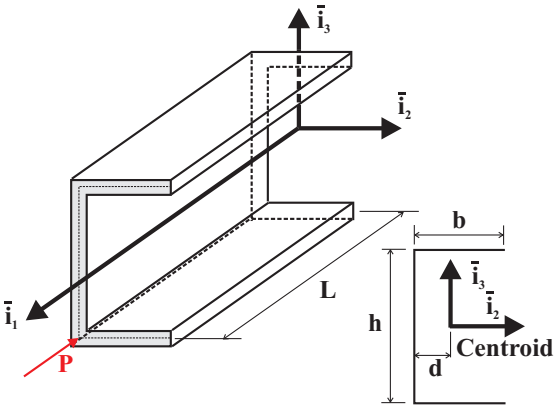

Fig. 14.25. Cantilevered beam with a C-channel cross-section.

Problem 14.11. Cantilevered beam with a C-channel cross-section

A uniform cantilevered beam with a thin-walled, C-channel cross-section is subjected to an end compressive load P in the lower corner, as depicted in fig. 14.25. Let $L = 10b$, $h = 2b$, and $b = 10t$, where t is the constant wall thickness. *(1)* Find the distributions of transverse displacements $\bar{u}_2(x_1)$ and $\bar{u}_3(x_1)$. *(2)* Determine the buckling load $P_{\rm cr}$ of the system. *(3)* Plot $P/P_{\rm cr}$ versus $\bar{u}_2^{\rm tip}/b$ and $P/P_{\rm cr}$ versus $\bar{u}_3^{\rm tip}/b$, both on the same graph. $\bar{u}_2^{\rm tip}$ and $\bar{u}_3^{\rm tip}$ are the tip transverse displacements of the beam along the $\bar{\imath}_2$ and $\bar{\imath}_3$, respectively.

Problem 14.12. Cantilevered beam under tip tensile force

Consider a cantilevered beam of length L and bending stiffness H_{33}^c subjected to a tip transverse load, P, and a tip *tensile* axial force, F. The tip deflection of the beam will be denoted $\delta = \bar{u}_2(x_1 = L)$. The beam features a rectangular cross-section of width b and height h. *(1)* Compute the non-dimensional transverse displacement field $H_{33}^c\bar{u}_2(\eta)/PL^3$, where $\eta = x_1/L$ is the non-dimensional span-wise variable. Express your result in terms if the non-dimensional axial force factor $\lambda = \pi/2\sqrt{F/P_{\rm Euler}}$, where $P_{\rm Euler} = \pi^2 H_{33}^c/4L^2$ is the buckling load for the cantilevered beam. *(2)* Compute the non-dimensional tip transverse displacement $H_{33}^c\delta/PL^3$. Show that for vanishing axial force, $F = 0$, the tip deflection becomes $\delta_0 = PL^3/(3H_{33}^c)$, as expected. *(3)* Plot the non-dimensional tip deflection δ/δ_0 as a function of $F/P_{\rm Euler} \in [0, 5.0]$. *(4)* On one graph, plot the non-dimensional transverse displacement field, $H_{33}^c\bar{u}_2(\eta)/(PL^3)$, for $F/P_{\rm Euler}$ = 0.0, 1.0, 2.0, 3.0, 4.0 and 5.0. *(5)* Plot the non-dimensional root bending moment $M_{\rm root}/(PL)$ as a function of $F/P_{\rm Euler} \in [0, 5.0]$. *(6)* On one graph, plot the non-dimensional bending moment distribution, $M_3(\eta)/(PL)$, for $F/P_{\rm Euler}$ = 0.0, 1.0, 2.0, 3.0, 4.0 and 5.0. *(7)* Based on simple statics arguments, prove that $M_{\rm root} = PL - F\delta$. Does your solution satisfy this relationship? *(8)* Plot the maximum root axial stress, σ/σ_0, as a function of $F/P_{\rm Euler} \in [0, 5.0]$. $\sigma_0 = 6PL/(bh^2)$ is the maximum root axial stress for a vanishing axial force, $F = 0$. Your result should depend on δ_0/h; select values of δ_0/h = 0.5, 1.0, 2.0, 3.0, 4.0 and 5.0. Is it possible to reduce the maximum axial stress in the cantilevered beam by applying the axial force F? Discuss your results.

Problem 14.13. Simply-supported beam under thermal loading

Consider a simply-supported beam of length L subjected to the parabolic thermal field depicted in fig. 14.26. The beam features a rectangular cross-section of height h and width b, where $h < b$. *(1)* Find the transverse deflection of the beam. *(2)* Find the critical thermal strain, $\alpha T_{\rm cr}$, at which the beam buckles. *(3)* Plot $T_0/T_{\rm cr}$ as a function of the beam's mid-span deflection, $\bar{u}_2^{\rm mid}/h$. *(4)* Plot $T_0/T_{\rm cr}$ as a function of the mid-span bending moment, $hM_3^{\rm mid}/H_{33}^c$. *(5)* How does the situation change if $h > b$?

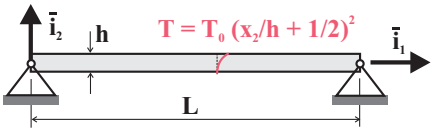

Fig. 14.26. Simply-supported beam under thermal loading.

14.3 Buckling of sandwich beams

Beams with sandwich cross-section are very common in aerospace constructions due to their high stiffness and strength to weight ratios. A typical sandwich cross-section is depicted in fig. 14.27. Two thin faces of thickness t_f and Young's modulus E_f sandwich a rather thick core of thickness t_c and Young's modulus E_c. The stiffness of the core is, in general, much smaller than that of the faces, $E_c \ll E_f$.

The bending stiffness of the complete sandwich section is readily found as

$$H^s_{33} = 2\frac{bt_f^3}{12}E_f + 2bt_f\frac{h^2}{4}E_f + \frac{bt_c^3}{12}E_c = bt_f\frac{h^2}{2}E_f\left[1 + \frac{1}{3}\frac{t_f^2}{h^2} + \frac{1}{6}\frac{t_c}{t_f}\frac{t_c^2}{h^2}\frac{E_c}{E_f}\right].$$

For typical constructions, the faces are much thinner than the core, $t_f/h \ll 1$, and the core material is very much softer than that of the faces, $E_c/E_f \ll 1$. Consequently, the bending stiffness reduces to

$$H^s_{33} \approx bt_f\frac{h^2}{2}E_f. \tag{14.54}$$

Very stiff constructions can be obtained by selecting deep cores (large values of h) and a stiff material for the faces (such as composite materials). Note that for a given amount of material, *i.e.*, for a specific face thickness t_f, the bending stiffness of the sandwich increases quadratically with the depth h.

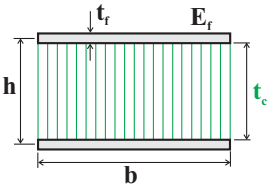

Fig. 14.27. Cross-section of a sandwich beam.

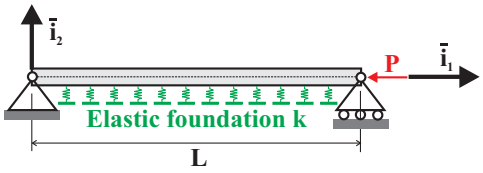

Fig. 14.28. Upper face of a sandwich structure under end compressive loads. The core of the sandwich is modeled by an elastic foundation.

If sandwich beams are subjected to axial compressive loads, buckling will occur when the critical load level is reached, *i.e.*, when $P_{\text{cr}} = \pi^2 H^s_{33}/L^2$ for a simply-supported boundary conditions. Because sandwich structures are designed to achieve large bending stiffnesses, they are efficient at sustaining large in-plane compressive loads.

This general instability of the structure is not the only failure mode of sandwich constructions. Because the core material is typically very soft, it carries a negligible portion of the axial force, and hence, the axial compressive load is primarily carried by the thin faces. Figure 14.28 shows an idealized model of the upper face of the sandwich subjected to an axial compressive load P. If a sandwich beam is subjected

to an axial force N_1, the load in each of the upper and lower faces will be $P \approx N_1/2$, assuming identical faces and a negligible contribution of the core to supporting the axial force.

Although the core material is of little help in carrying the axial compressive load, it does provide an elastic support for the faces. This elastic support can be approximated by an elastic foundation of stiffness constant k, as depicted in fig. 14.28. The problem is now to determine the buckling load of the system shown in fig. 14.28, which consists a beam acted upon by axial compressive forces and resting on an elastic foundation of stiffness k. The bending stiffness of the face, $H_{33}^f = E_f b t_f^3/12$, is much smaller than that of the sandwich beam given by eq. (14.54), and hence its buckling load can be considerably lower than that of the sandwich beam.

The buckling problem for the thin face resting on an elastic foundation will be treated using an energy approach with the following assumed displacement field for the face

$$\bar{u}_2(x_1) = \sum_{n=1}^{\infty} q_n \sin \frac{n\pi x_1}{L},$$

where q_n are unknown displacement parameters. Note that each assumed displacement mode, $\sin n\pi x_1/L$ satisfies the geometric boundary conditions of the problem.

The total potential energy of the system is

$$\Pi = \frac{1}{2}\int_0^L H_{33}^f \left(\frac{\mathrm{d}^2\bar{u}_2}{\mathrm{d}x_1^2}\right)^2 \mathrm{d}x_1 + \frac{1}{2}\int_0^L k\,\bar{u}_2^2\,\mathrm{d}x_1 - \frac{1}{2}\int_0^L P\left(\frac{\mathrm{d}\bar{u}_2}{\mathrm{d}x_1}\right)^2 \mathrm{d}x_1,$$

where the first term represents the strain energy associated with the bending of the face, the second term the strain energy in the elastic foundation, and the last term the work done by the axial compressive load P. Introducing the assumed displacement field in this expression leads to

$$\begin{aligned}\Pi = {} & \frac{H_{33}^f}{2}\sum_{m=1}^{\infty}\sum_{n=1}^{\infty} q_m q_n \left(\frac{m\pi}{L}\right)^2\left(\frac{n\pi}{L}\right)^2 \int_0^L \sin\frac{m\pi x_1}{L}\sin\frac{n\pi x_1}{L}\,\mathrm{d}x_1 \\ & + \frac{k}{2}\sum_{m=1}^{\infty}\sum_{n=1}^{\infty} q_m q_n \int_0^L \sin\frac{m\pi x_1}{L}\sin\frac{n\pi x_1}{L}\,\mathrm{d}x_1 \\ & - \frac{P}{2}\sum_{m=1}^{\infty}\sum_{n=1}^{\infty} q_m q_n \left(\frac{m\pi}{L}\right)\left(\frac{n\pi}{L}\right) \int_0^L \cos\frac{m\pi x_1}{L}\cos\frac{n\pi x_1}{L}\,\mathrm{d}x_1.\end{aligned}$$

In view of the orthogonality of trigonometric functions, see apendix A.4, the total potential energy reduces to

$$\Pi = \frac{1}{2}\sum_{m=1}^{\infty}\left[H_{33}^f\left(\frac{m\pi}{L}\right)^4 + k - P\left(\frac{m\pi}{L}\right)^2\right]\frac{L}{2}q_m^2.$$

The principle of minimum total potential energy implies that Π is a minimum with respect to the choice of the displacement parameters q_m. Hence $\partial\Pi/\partial q_n = 0$, for $n = 1, 2, \ldots \infty$ or

$$\left[H_{33}^f \left(\frac{n\pi}{L}\right)^4 + k - P\left(\frac{n\pi}{L}\right)^2\right] q_n = 0, \qquad n = 1, 2, \ldots \infty.$$

This represents a set of homogeneous, uncoupled algebraic equations for the unknown displacement parameters q_n. The solution of this system is $q_n = 0$, $n = 1, 2, \ldots \infty$, corresponding to the trivial solution of the problem. A non-trivial solution exists if and only if the determinant of the system of equations vanishes, leading to the following condition

$$H_{33}^f \left(\frac{n\pi}{L}\right)^4 + k - P\left(\frac{n\pi}{L}\right)^2 = 0, \quad n = 1, 2, \ldots \infty.$$

Solving for the critical load yields

$$P_{\mathrm{cr}\,n} = H_{33}^f \left(\frac{n\pi}{L}\right)^2 + k\left(\frac{L}{n\pi}\right)^2 = \frac{\pi^2 H_{33}^f}{L^2}\left[n^2 + \frac{kL^4}{\pi^4 H_{33}^f}\frac{1}{n^2}\right], \quad n = 1, 2, \ldots \infty.$$

In this expression, $P_{\mathrm{Euler}} = \pi^2 H_{33}^f / L^2$ is the Euler buckling load for the simply-supported face in the absence of elastic foundation. If $\bar{k} = kL^4/\pi^4 H_{33}^f$ is defined as the non-dimensional stiffness of the elastic foundation, the critical loads of the system become

$$\frac{P_{\mathrm{cr}\,n}}{P_{\mathrm{Euler}}} = n^2 + \frac{\bar{k}}{n^2}, \qquad n = 1, 2, \ldots \infty.$$

Each of the above critical loads gives rise to a non-trivial solution of the problem, and the lowest critical load is the buckling load. The lowest critical load, however, is not always obtained for $n = 1$; indeed, as n increases, the first term, n^2, increases, but the second term, $\bar{k}/n^2$, decreases. This implies that the wave number, n, that yields the lowest critical load is itself a function of $\bar{k}$.

To illustrate this point, fig 14.29 shows the non-dimensional critical loads $P_{\mathrm{cr}\,n}/P_{\mathrm{Euler}}$ for $n = 1$, 2, and 3. For a wave number $n = 1$, the critical load is $P_{\mathrm{cr}\,1}/P_{\mathrm{Euler}} = 1 + \bar{k}$, a linear relationship. For $n = 2$, the critical load is $P_{\mathrm{cr}\,2}/P_{\mathrm{Euler}} = 4 + \bar{k}/4$, which is also a linear relationship, and defines a dashed line with intermediate slope. A third dashed line is shown for $n = 3$. It follows that when $0 \le \bar{k} \le 4$, the lowest critical load is obtained for a wave number $n = 1$ but when $4 \le \bar{k} \le 36$, the lowest critical load is obtained with $n = 2$. The buckling load is therefore a function of $\bar{k}$, and it consists of an envelope of straight line segments, each with a different value of the wave number.

Let $\bar{k}_{\mathrm{co}}$ be the cross-over value of $\bar{k}$ at which the wave number switches from n to $n+1$. This cross-over point is the intersection of two straight lines, $P_{\mathrm{cr}\,(n)}/P_{\mathrm{Euler}} = n^2 + \bar{k}/n^2$ and $P_{\mathrm{cr}\,(n+1)}/P_{\mathrm{Euler}} = (n+1)^2 + \bar{k}/(n+1)^2$, which is readily found as $\bar{k}_{\mathrm{co}} = n^2(n+1)^2$. It follows that the range of values of $\bar{k}$ for which buckling occurs with wave number n is

$$(n-1)^2 n^2 \le \bar{k} \le n^2 (n+1)^2.$$

When looking at a large range of values of $\bar{k}$, the various straight line segments blend together into a smooth curve, as illustrated in fig. 14.30. The buckling load can then

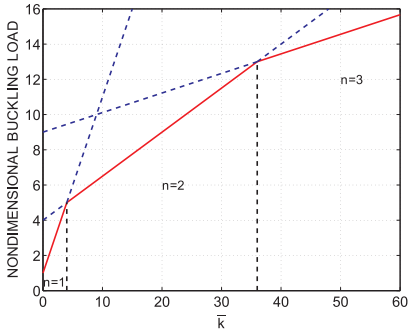

Fig. 14.29. Non-dimensional critical loads $P_{\mathrm{cr}\,n}/P_{\mathrm{Euler}}$ for n = 1, 2, and 3.

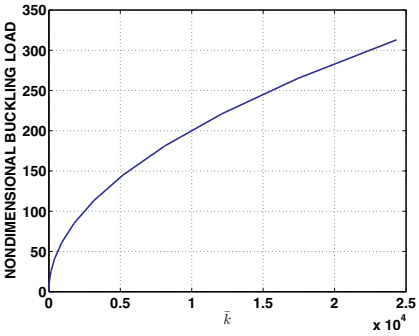

Fig. 14.30. Non-dimensional buckling load $P_{\mathrm{cr}}/P_{\mathrm{Euler}}$ versus $\bar{k}$.

be approximated as $P_{\mathrm{cr}}/P_{\mathrm{Euler}} \approx 2\sqrt{\bar{k}}$. This result, however, hides the constantly changing wave number as the elastic foundation stiffness $\bar{k}$ changes.